Photodiagnosis and Photodynamic Therapy 28 (2019) 330–337

Contents lists available at ScienceDirect

Photodiagnosis and Photodynamic Therapy

journal homepage: www.elsevier.com/locate/pdpdt

Antibacterial photodynamic therapy mediated by 5-aminolevulinic acid on methicillin-resistant *Staphylococcus aureus*

Jianhua Huang[a], Mingquan Guo[b], Shengkai Jin[c], Minfeng Wu[a], Chen Yang[c], Guolong Zhang[c], Peiru Wang[c], Jie Ji[c], Qingyu Zeng[c], Xiuli Wang[c], Hongwei Wang[a,*]

[a] Department of Dermatology, Huadong Hospital, Fudan University, Shanghai 200040, PR China
[b] Shanghai Institute of Bacteriophage and Drug Resistance, Shanghai Public Health Clinical Center, Fudan University, Shanghai 201514, PR China
[c] Shanghai Skin Disease Hospital, Institute of Photomedicine, Tongji University School of Medicine, Shanghai, PR China

ARTICLE INFO

Keywords:
Drug resistance
Staphylococcus aureus
MRSA
5-aminolevulinic acid
Photodynamic therapy
Antimicrobial Photdynamic Therapy

ABSTRACT

The emergence of drug-resistant bacteria, such as methicillin-resistant *Staphylococcus aureus* (MRSA), has brought great difficulties to clinical treatment. Antibacterial photodynamic therapy (aPDT) is a new non-antibiotic treatment strategy for a variety of drug-resistant bacteria. However, there are few studies on the antimicrobial mechanism of a PDT mediated by 5-aminolevulinic acid (ALA-PDT) for MRSA. In this study, we observed the bactericidal effect of ALA-PDT on MRSA. We found that ALA-PDT had the strongest bactericidal effect when ALA was at 0.05 mM, and the bactericidal activity of aPDT increased with the increase of light dose. MRSA was almost completely eliminated at 0.05 mM and 384 Jcm^{-2}. In addition, the bactericidal morphology was also observed under a fluorescence microscope using a LIVE/DEAD® BacLight™ Bacterial Viability Kit and an electron microscope. It was also found that proteins and DNA were damaged by ALA-PDT. Finally, the transcription level of the specific gene of MRSA, *nuc*, was decreased by 0.74-fold ($P < 0.05$) after ALA-PDT treatment by qRT-PCR analysis. The findings suggest that ALA-PDT can effectively inhibit MRSA by damaging cell membrane, cytoplasm, proteins and nucleic acid.

1. Introduction

Staphylococcus aureus is widely distributed in nature. Most of the *S. aureus* do not cause diseases, but a few can cause suppurative infections of humans and animals, mainly including carbuncle, folliculitis, pneumonia, brain abscess, liver abscess, suppurative osteomyelitis and wound infections [1–4]. It is a major cause of community acquired and nosocomial pathogenic bacteria, which was associated with many severe infections and high mortality rate [5]. Methicillin-resistant *S. aureus* (MRSA), the resistant strain of *S. aureus* due to overuse of antibiotics and other reasons, has brought greater difficulties to treatment [6]. Vancomycin is commonly used as a last resort to control MRSA infections, however, worldwide reports indicate that the extensive use of vancomycin has led to a growing trend of vancomycin resistance [6]. MRSA has heterogeneous and broad-spectrum drug resistance. Currently, there is no effective way to deal with MRSA infections clinically. The mean length of hospital stay (3.95 v 2.36 days; $P < 0.05$) and mortality (almost 50% higher) of patients infected with MRSA were significantly increased, compared with that of other patients [7,8]. This poses a serious challenge for clinicians to treat MRSA infections, and new antimicrobial strategies are urgently needed to combat MRSA.

aPDT was regarded as an adjunctive therapy and novel non-antibiotic strategy for various antibiotic-resistant bacteria [5]. aPDT involves the synergistic action of visible or near-infrared light with non-toxic photosensitizers (PSs) and oxygen, thus forming cytotoxic reactive oxygen species (ROS) to destroy target organisms (such as bacteria, viruses, fungi, etc.) [9]. Compared with traditional antibiotic therapy, aPDT has a wide range of functions, and is more toxic to bacteria than mammalian cells, killing bacteria without interfering with host tissues [10,11]. Unlike antibiotics, aPDT does not induce bacteria resistance, and bacteria can be treated repeatedly [12,13]. In addition, aPDT mainly targets the local illumination area of inflammation, which causes less systemic response [14]. Recently, photodynamic inactivation (PDI) has drawn more attention due to its local antibacterial effect. Several studies have reported the efficacy of PDI on gram-positive and gram-negative planktonic and biofilm bacteria in vitro and in vivo

* Corresponding author.
E-mail addresses: 281284528@qq.com (J. Huang), gmqjiandan@163.com (M. Guo), jinsk1223@163.com (S. Jin), 996392167@qq.com (M. Wu), yangchen1259@163.com (C. Yang), zglamu@163.com (G. Zhang), wpeiru@qq.com (P. Wang), jier_2006@163.com (J. Ji), xiaojinyuhen@126.com (Q. Zeng), xlwang2001@aliyun.com (X. Wang), hongweiwang2005@aliyun.com (H. Wang).

https://doi.org/10.1016/j.pdpdt.2019.09.008
Received 27 June 2019; Received in revised form 10 September 2019; Accepted 27 September 2019
Available online 13 October 2019

[15–19]. Researchers conducted studies on the inhibitory effect of ALA-PDT on *Staphylococcus epidermidis* in vitro, which confirmed that ALA-PDT had a significant inhibitory effect on *S. epidermidis* [20].

5-aminolevulinic acid (ALA), a natural photosensitizer (PSs) prodrug, is converted to protoporphyrin IX (PpIX) in target cells [21]. Compared with other PSs, ALA is a natural intermediate in the heme biosynthesis pathway and can be rapidly removed from target cells [22]. More importantly, it is small enough to penetrate the matrix and accumulate in the target cells with lower toxicity [23]. However, there are few studies on the antimicrobial mechanism of ALA-PDT on MRSA, and the previous parameters are different. Therefore, it is an urgent need to monitor the safe and effective germicidal parameters of ALA-PDT and discuss its antimicrobial mechanism against MRSA. In this work, we assessed the antibacterial effect of ALA-PDT on antibiotic-resistant bacterial planktonic strain of MRSA in vitro and further evaluated its bactericidal mechanism. Our findings may provide an experimental basis for future clinical application of ALA-PDT on MRSA infections.

2. Materials and methods

2.1. MRSA strain and culture conditions

The MRSA SA325 strain was kindly provided by PhD Mingquan Guo at Shanghai Public Health Clinical Center. The culture of bacteria followed the previous methods [17]. Briefly, the strain was grown in Luria–Bertani (LB) medium including liquid medium, solid medium (1.5% agar) at 37 °C. 50 μL of the culture was transferred into 5-mL fresh LB and incubated at 37 °C to logarithmic phase, optical density (OD) at 600 nm of 0.8 (corresponding to 5×10^8 colony forming units (CFU) mL^{-1}). The pellets were collected by centrifugation at 8000 rpm for 5 min using the centrifuge (Fresco21, USA) and washed three times with sterilized phosphate-buffered saline (HyClone SH30256.01B). The pellets were resuspended with PBS to the same concentration (OD 600 nm of 0.8) using a UV–vis spectrophotometer (G6860A, Malaysia) prior to experiments. For preservation of bacteria, bacteria in LB culture at logarithmic phase were stored with equal volume of glycerin (50%) at −20 °C.

2.2. Photosensitizer and light source

ALA was purchased from Fudan Zhanjiang Bio-Pharm, Shanghai, China. A 100 mM stock solution was freshly prepared by dissolving in PBS and adjusted to neutral pH 7.2 with NaOH. The stock solution was filtered through a 0.22-μm filter disk (MILLEX GP SLGP033RB, USA) and stored in the dark at 4°C. All the illuminations experiments were performed with a light-emitting diode array (LED-IB, China) at a wavelength of 633 ± 10 nm as the light source in this study. The output power capacity at the level of the samples was 406 mW cm^{-2}, as measured with a power meter (SJG-2000 mW, China). The central illumination area (about 4.6 cm in diameter) was regarded as the experimental region.

2.3. Uptake of ALA in MRSA

Various concentrations of ALA solutions were prepared, added into bacterial suspension to final varying concentrations (0–50 mM), and then incubated in the dark at 37℃ for 1 ~ 12 h (0 mM as the negative control). The cells were collected by centrifugation and rinsed three times with PBS. Then, fluorescence in cells was measured with a microplate reader (SpectraMax M2, USA) at 1 h, 4 h, 12 h to show the biological synthesis of porphyrins into the bacterial strain. The amounts of ALA binding to bacterial cells were determined in cell suspensions incubated with different concentrations of ALA. The excitation wavelength was 410 nm and the emission spectra of the solutions were recorded at 630 nm.

2.4. Dark toxicity of ALA and phototoxicity of light on MRSA

Toxicity of ALA and phototoxicity of light were assayed according to the previously described with some adjustments [24]. Briefly, bacterial suspensions of MRSA at logarithmic phase were incubated with ALA at various concentrations (0, 0.005, 0.05, 0.5, 5, 50 mM) in the dark for 1 h, 4 h and 12 h at 37 °C. To evaluate phototoxicity activity, irradiation was applied using an LED emitting visible light with 633 ± 10 nm for 0 Jcm^{-2}, 96 Jcm^{-2}, 192 Jcm^{-2}, 384 Jcm^{-2}. Thereafter, bacterial suspensions were serially diluted 10-fold with PBS, and 100 μL of diluent was then collected and coated on a LB agar plate [17]. After incubation overnight at 37 °C, the toxicity of ALA and phototoxicity of light were calculated by counting CFUs. Log-transformation of CFU mL^{-1} was performed before statistical analysis.

2.5. aPDT on bacteria and HaCat in vitro

Aliquots (100 μL) of the MRSA suspensions in a final concentration of 5×10^8 CFU mL^{-1} in PBS were inoculated into a 96-well plate (Corning, USA), mixed with equal volumes ALA of different concentrations (0–50 mM), and then incubated in the dark at 37 °C for different time. The samples were divided into four groups: L − S− (control), L + S−, L − S+, L + S+ (L: Light; S: Sensitizer). For the ALA alone and control group, bacterial suspensions were mixed with equal volumes of PBS. The laser groups were irradiated with a total light energy of 96 Jcm-^{2}, 192 Jcm-^{2}, 384 Jcm-^{2}, respectively. In the aPDT group, samples were incubated with the indicated concentrations of ALA in the dark and then were illuminated as the laser group. To avoid heating of the samples, the 96-well was placed on ice during illumination. The light device was held in a fixed vertical position of 5 mm above the top plate to maintain the light energy delivered to the samples equal in all the experiments. Then, viable bacteria were quantified by the colony counting method described as above. For the aPDT phototoxicity to normal mammalian cells, same experiment was performed on HaCat cell line, and then, survival fraction was detected via cell counting kit 8 (CCK-8) assay (Beyotime Biotechnology, Shanghai, China). In all the experiments, the room temperature was kept at about 25℃.

2.6. Measurement of ROS

In order to verify whether ROS is produced in the process of bactericidal effect by aPDT, intracellular ROS levels were monitored by a microplate reader (SpectraMax M2, USA) according to the previous study with some adjustments [25]. Briefly, the ROS generation were probed with 2, 7-dichlorofluorescein diacetate (DCFH-DA). Treated bacteria were incubated with 10 μM DCFH-DA in the dark at 37℃ for 30 min. After the co-incubation, the cells were washed with PBS three times, and the fluorescence intensity was immediately measured.

2.7. Bacteria-viability assay

Bacterial viability was analyzed by a fluorescence microscopy (BX51TF, Olympus) with a LIVE/DEAD® BacLight™ Bacterial Viability Kit (Invitrogen L13152). Briefly, MRSA cells were harvested and resuspended in PBS to 5×10^8 CFU mL^{-1}. A mixture of dyes was added to the samples and kept for 30 min in dark. Stained bacterial cells were visualized at excitation/emission wavelengths of about 485/500 nm for SYTO 9 and 535/617 nm for propidium iodide (PI) under the fluorescence microscopy.

For the morphologic observation, transmission electron microscopy (TEM) was employed to detect cytoplasmic decomposition. Bacterial suspensions were pelleted by centrifuging at 4000 rpm for 10 min and the pellets were fixed in 2.5% glutaraldehyde (SCRC, China), washed once in PBS, and post-fixed in 1% osmium tetroxide (Pelco, USA). Afterwards, the pellets were dehydrated and embedded in Epon 812

epoxy resin (SPI-Chem, USA). Finally, the samples were viewed and digitally photographed using a TEM (Hitachi H-7650, Japan). Five images of each MRSA strain were randomly chosen from different perspective and blinded to observe.

2.8. DNA extraction and gel electrophoresis

The bacterial DNA from different groups was prepared and analyzed by agarose gel electrophoresis to evaluate genomic DNA damage. Bacterial DNA was harvested using a DNA extraction kit (QIAGEN, Germany). Agarose (0.3 g) was suspended in 1 × TAE (Tris/acetate/EDTA) buffer (30 mL) and heated to boiling point. The solution was allowed to cool to 60℃ prior to the addition of 1 μL of Gelred (Biotium, USA) and then mixed thoroughly. The DNA extraction products (5 μL) mixed with 6 × loading buffer (1 μL) was added into each well. The DNA fragments from the untreated and treated with light and/or ALA can be separated and visualized by agarose gel electrophoresis. Quantitation of DNA band intensity was performed by the Image J software, which transformed the band intensity into a form of area without unit. Area values could be used to compare the relative differences of intensity levels among groups [26].

2.9. Proteins extraction and analysis

SDS-PAGE (sodium dodecyl sulfate polyacrylamide gel electrophoresis) was employed to confirm whether ALA-PDT destroyed cell proteins. Samples from different groups were washed three times in PBS. The suspension of the collected pellets in 40 μL RIPA Buffer (pierce 89900) was sonicated in a 1.5 mL Eppendorf tube and the protein was quantified by BCA assay. 10 μL of 5 × SDS gel-loading buffer was added into each sample. After heating at 95°C for 10 min, samples were centrifuged at 12,000 rpm for 2 min at 4°C and an aliquot (5 μL) of the centrifugal supernatant was loaded on a 12.5% SDS polyacrylamide gel made with a rapid preparation of PAGE gel kit (Epizyme, China). The gel was run at 8 Vcm^{-1} and then dyed with Coomassie Blue Fast Staining and No-decoloring Solution Kit (Epizyme, China). The analysis of protein gray intensity was the same as that of DNA electrophoresis.

2.10. Evaluation of the expression of nuc gene following treatment by relative quantitative real time PCR (qRT-PCR)

To determine changes of the specific gene (*nuc*) of ALA-PDT-treated MRSA strains, *nuc* gene expression was quantitated with qRT-PCR according to the previous study [27]. Briefly, after treatment, total RNA of the MRSA suspension was extracted with RNA extraction kit (PureLink™ RNA Mini Kit, Invitrogen) as described by the manufacturer's instructions. RNA quantity and quality were determined using NanoDrop™ 2000 spectrophotometer (Thermo Scientific, USA) with an A260/A280 ratio. Afterwards, genomic DNA was removed by RNase-free DNase I reagent. qRT-PCR was performed using a three-step reaction for the quantification of *nuc* gene mRNA levels. RNA was converted to cDNA using a Hifair®II 1 st Strand cDNA Synthesis SuperMix for qPCR (gDNA digester plus) Kit (Yeasen, China) as described by the manufacturer instructions. Target gene primers and internal control sequences were found from previous studies and synthesized by Shanghai Sunny Biotechnology Co, Ltd. The *nuc* genes primers were F-forward 5′-CAAAG CATCAAAAAGGTGTAGAGA-3′ and R-forward 5′-TTCAATTTTCTTTGC ATTTTCTACCA-3′, and *16S rRNA* primers : F-forward 5′-AGAGTTTG ATCCTGGCTCAG-3′, R-forward 5′-ACGGCTACCTTGTTACGACTT-3′ [28,29]. qRT-PCR was carried out in a volume of 50 μL reaction mixture with a Hieff qPCR SYBR® Green Master Mix (No Rox) Kit (Yeasen, China) under thermal cycling conditions: an initial denaturation at 95℃ for 5 min; 40 cycles of denaturation (95℃, 10 s), annealing (55–60°C, 20 s) and prolongation (72°C, 20 s), then 1 cycle of melting curve analysis (95°C, 15 s; 60°C, 60 s; 95°C, 15 s). The fold changes of *nuc* transcription levels were calculated by the $2^{-\Delta\Delta Ct}$ method using the QIAGEN 2009 Relative Expression Software Tool (REST).

2.11. Data analysis

Data were expressed as mean ± SEM. The normality distribution and homogeneity of the data was confirmed by the Kolmogorov-Smirnov test and Brown-Forsythe test, respectively. Statistical analyses were evaluated using the one-way analysis of variance (ANOVA) followed by Tukey post hoc test for pairwise comparisons. All analyses were performed using GraphPad Prism 8.0.1. All the experiments above were performed in triplicate, and P values < 0.05 were considered as statistically significant. Significance in data with respect to their controls were represented by asterisk sign (*) in the bar graphs.

3. Results

3.1. Uptake of PSs and ALA dark toxicity and phototoxicity

The uptake of ALA generally corresponds to the sensitivity of MRSA strain SA325 to aPDT. The uptake experiment showed that except for 0 mM, the fluorescence intensity of all other concentrations increased with time and the accumulated amounts were comparable at the same time. As shown in Fig. 1A, 0 mM as control, fluorescence intensity increased by 3.21–6.38 folds, 12.08–24.39 folds and 34.59–52.72 folds at 1, 4 and 12 h, respectively. Interestingly, fluorescence intensity did not increase with the increase of ALA concentrations and reached the peak at 0.05 mM, while it was relatively weak at 0.005 mM and 50 mM. Then, the dark toxicity of ALA and the phototoxicity of light alone to MRSA was analyzed. Within 4 -h incubation, the number of colonies incubated at all concentrations did not decrease (Fig. 1A). However, toxicity was found after 12 -h incubation at or above 5 mM, but not in the groups less than 5 mM (Fig. 1B). In addition, the phototoxicity of MRSA SA325 to the direct exposure was also tested (Fig. 1C). Without ALA, the phototoxic effects of different light doses on CFU of bacterial SA325 showed little difference.

3.2. Optimal incubation time

We chose all tested concentrations of ALA with 1 and 4 h of incubation, followed by the minimum illumination of 96 Jcm^{-2}. As shown in Fig. 2, when ALA concentration and the light dose were constant, the bactericidal effect of aPDT was dependent on incubation time (Fig. 2A). Compared with other concentrations, 0.05 mM ALA showed the most bactericidal effect with reduction of 3.3 log after 4 h of incubation, while ALA showed no significant cytotoxic effect at any concentration after 1 h incubation. Thus, according to the results of PDI efficacy, 4 h of incubation time is ideal. So 4 h was adopted as the optimal incubation time in the further experiments.

3.3. aPDT on MRSA and HaCat

The fraction at 0.05 mM showed the most reduced bacterial survival among all tested concentrations at the same illumination energy. As shown in Fig. 2, when the concentration ranged from 0 mM to 0.05 mM, the bacterial survival rate decreased with the increase of concentration. As the concentration increased further, the bacteriostatic activity became weakened. For example, at 384 Jcm^{-2}, the viable bacteria treated by 0.005 mM, 0.05 mM, 0.5 mM, 5 mM and 50 mM decreased by 0.65 log, 8.47 log, 3.44 log, 0.62 log and 0.40 log, respectively. Furthermore, ALA decreased bacteria growth in a light dose-dependent manner. 0.05 mM ALA at 384 Jcm^{-2} yielded complete elimination of bacteria, indicating that all tested cells were inactivated (Fig. 2B). Under 96 Jcm^{-2} and 192 Jcm^{-2}, ALA-PDT inactivated 1.31% and 0.09% of MRSA respectively, while HaCaT cells were safe. However, when the energy increased to 384 Jcm^{-2}, 100% of MRSA died and about 30.03% of HaCat cells survived (Fig. 2C).

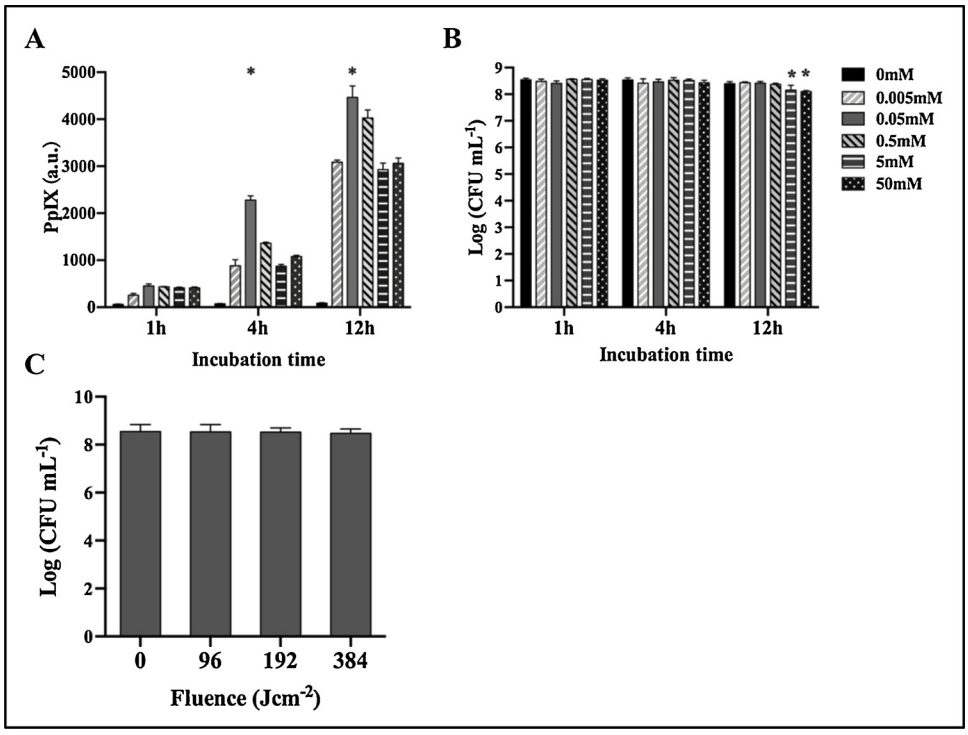

Fig. 1. Uptake of PSs, dark toxicity of ALA and light phototoxicity to planktonic MRSA were analyzed. (A) At incubation time point of 1, 4, 12 h, the uptake of 0.005 mM, 0.05 mM, 0.5 mM and 5 mM ALA in MRSA SA325 was higher than that of 0 mM ALA. (B) Dark toxicity was showed with statistic difference above 5 mM ALA after 12 -h incubation. (C) No significant phototoxicity of 0, 96, 192, 384 Jcm^{-2} fluence on planktonic MRSA was found. All data were expressed as mean ± SEM (n = 3). *, $P < 0.05$ is significantly different from the 0 mM groups.

3.4. Bacteria-viability analysis

The inflow of SYTO 9 and PI was observed to analyze the ability of ALA-PDT to damage the cell membrane. Fig. 3A and B showed there was a decline in the ratio of green/red fluorescence intensity in the aPDT group compared with other groups. The results demonstrated that the number of live cells (green) decreased and the number of dead cells (red) increased in the aPDT group. Similar to the untreated group, the majority of cells showed green fluorescence in the light illumination alone and ALA alone groups.

As shown in the micrographs, in the control group, ALA alone and light alone groups, MRSA cells were round-shaped and the cell envelope was smooth and intact, the normally dividing bacterial cells were observed with dense cytoplasm staining and a few particles, which were evenly distributed. In contrast, in the aPDT group, the cell envelope was irregular, thinning, discontinuous, and even less well-defined. In addition, the images also showed highly variable cells, low nucleic acid content, partial devoid of intracellular contents, as well as leakage and damage to the cytoplasm (Fig. 3C).

3.5. Measurement of intracellular ROS production, proteins degradation and genomic DNA damage in MRSA following ALA-PDT

We found that exposure of MRSA to ALA-PDT significantly affects intracellular ROS levels. The aPDT group showed considerably higher ROS production than other three groups ($P < 0.05$). When compared with the L − S−, L + S−, L − S+ groups, the aPDT group showed remarkably increased fluorescence intensity by 138.61% ($P < 0.01$),

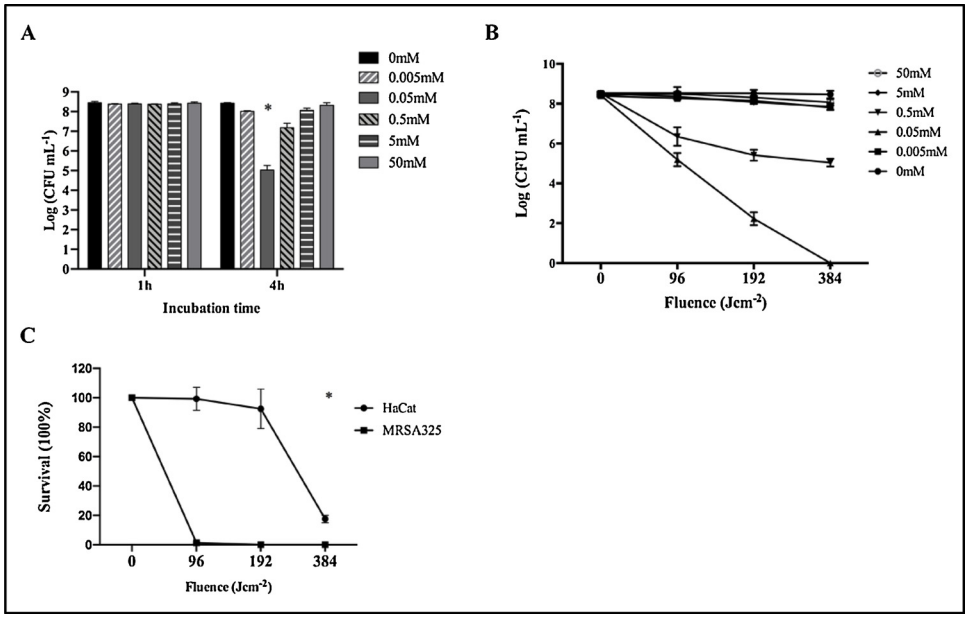

Fig. 2. (A) Under 96 Jcm^{-2} irradiation, viable MRSA colonies began to decrease significantly after incubation for 4 h at 0.05 mM. (B) Bacteria were completely inactivated at 384 Jcm^{-2} irradiation and 0.05 mM ALA after 4 h. (C) Under 96 Jcm^{-2} and 192 Jcm^{-2}, most MRSA cells were inactivated, while HaCat cells were not affected. All data were expressed as mean ± SEM (n = 3). * $P < 0.05$ means significantly different. from the controls (0 mM in A, 0 Jcm^{-2} in B, respectively).

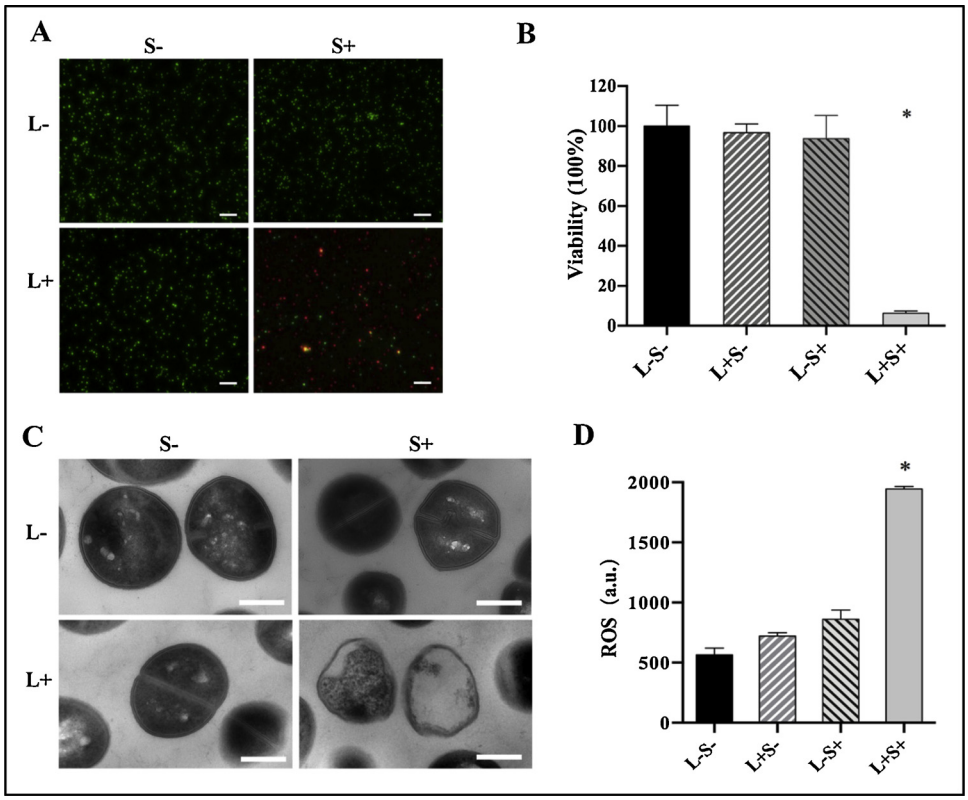

Fig. 3. Bacteria was incubated in presence of 0.5 mM ALA (S+) or PBS (S-), and then irradiated by 384 Jcm^{-2} (L+) or not (L−). (A, B) Coexistence of light and ALA showed most inhibition on bacteria, bar: 20 μm in A. Data were expressed as mean ± SEM (n = 5). (C) TEM images exhibited irregular cell envelope, low nucleic acid content and leakage to the cytoplasm, bar: 500 nm. Data were expressed as mean ± SEM (n = 5). (D) Combination of light and ALA produced largest amount of ROS. Data were expressed as mean ± SEM (n = 3). * $P < 0.05$ means significantly different from the controls (L−S−).

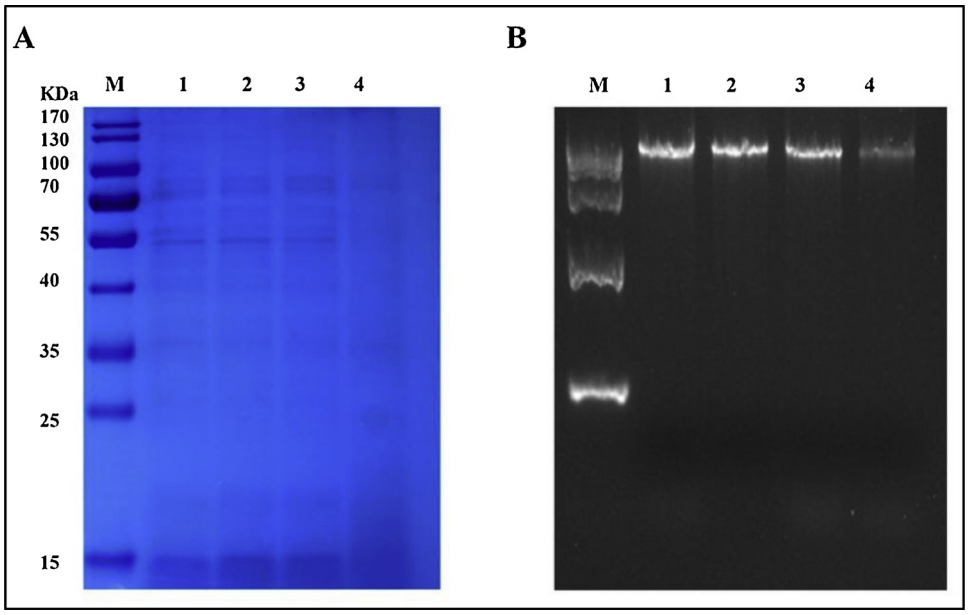

Fig. 4. (A) SDS-PAGE displayed the majority of proteins in bacteria were degraded after ALA-PDT (lane M, marker; lane 1, L–S–; lane 2, L + S−; lane 3, L − S+; lane 4, L + S+). (B) Agarose gel electrophoresis indicated obvious damage to genomic DNA in ALA-PDT group (lane M, DNA marker; lane 1, L-S-; lane 2, L + S-; lane 3, L-S+; lane 4, L + S+).

105.39% ($P < 0.01$) and 97.31% ($P < 0.01$), respectively (Fig. 3D). It was observed that cells irradiated without ALA also generated ROS as little as the untreated and the ALA alone group. SDS-PAGE was also performed to confirm whether ALA-PDT had significant degradation effects on cell proteins. The results of SDS-PAGE analysis showed that after ALA-PDT, the protein bands almost all disappeared (Fig. 4A). We selected a representative group of bands, which were well recognized at the position of 70 KDa, for gray intensity analysis. The intensity of L + S+ group was significantly reduced ($P < 0.01$), compared with that of L − S− (15,908.67 ± 1885.46), L + S− (12,303.33 ± 3145.65) and L − S+ (12,996.67 ± 1223.54) groups, without significant difference among the latter three groups ($P > 0.05$). Meanwhile, the detection results of bacterial genome damage showed that the L − S−, L + S− and L − S+ groups had higher molecular weight (17,672.19 ± 1842.76, 14,549.58 ± 788.25, 13,719.28 ± 1064.03, respectively, $P > 0.05$) than the aPDT treated group (4884.86 ± 438.82, $P < 0.01$), making the genome DNA band on the agarose gel very weak (Fig. 4B).

3.6. Analysis of *nuc* gene transcription level following ALA-PDT

Compared to the other three groups, the transcription level of *nuc* gene was altered by ALA-PDT, and REST software displayed a 0.74-fold decrease in the *nuc* mRNA transcription at a sub-lethal dose of aPDT-

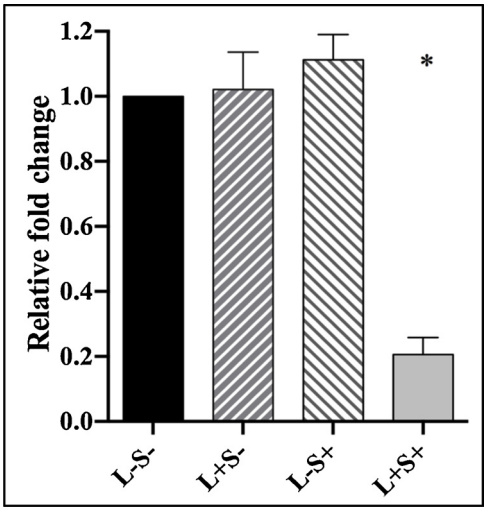

Fig. 5. qRT-PCR suggested that ALA-PDT could remarkably reduce *nuc* gene expression. Data were expressed as mean ± SEM (n = 3). *, P < 0.05 is significantly different from the control (strain grown without treatment).

treated MRSA (Fig. 5). The *nuc* gene transcription was relatively high without significant difference among the other three groups in control, ALA alone and light alone groups.

4. Discussion

The emergence of MRSA as a problematic hospital pathogen has aroused clinical concern. MRSA has become one of the important pathogens of hospital and community infection since its discovery [30,31]. When MRSA is isolated in clinic, vancomycin is the preferred drug. Unfortunately, the widespread use of vancomycin has also led to a worrying trend of increasing vancomycin resistance [6]. In recent years, the lack of an effective drug to eradicate MRSA infection has led the scientific community to use aPDT as an adjuvant treatment. Unlike conventional therapies, aPDT represents a multi-target damaging process, resulting in inactivation without the risk of the resistance development in PDI-induced oxidative stress [32]. Giuliani et al. [33] detected that no occurrence of drug resistance was found after 20 consecutive aPDT treatments. Based on its many advantages, aPDT was a promising method and widely used to treat various infections [34,35]. In this study, we mainly investigated the antimicrobial action and mechanism of ALA-PDT on MRSA.

The incubation time of PSs was a critical parameter for aPDT effect [36]. The optimal incubation time of ALA for aPDT was different in previous studies [19,24,37]. We found ALA could produce a large amount of PpIX after 4 h' incubation in the dark, which was consistent with Nitzan's research [38]. The fluorescence intensity of PpIX increased significantly after the concentrations of 0.005 mM–50 mM in the dark even for 1 h at 37℃, and the fluorescence became stronger with the prolongation of incubation time, which indicated ALA binding to bacterial cells increased with time. Interestingly, the maximal level of porphyrins was not found at the highest ALA concentration (50 mM), but peaked at the moderate ALA concentration (0.05 mM). This phenomenon generally corresponded well with a previous study, which found ALA maintained a plateau after reaching their maximal level of porphyrin [39]. The accumulation in cells became lower at high concentrations may be ascribed to the cell permeability change driven by high concentrations of ALA, causing higher release of PpIX [39]. In addition, the enzymes involved in the heme biosynthesis was generally inhibited by porphyrins to avoid the accumulation of large amounts of PpIX, and this negative feedback can result in a PpIX plateau as ALA concentration increases [40]. Our results also demonstrated that ALA itself seemed to inhibit porphyrin formation at higher concentrations, so that toxic drug concentrations could be avoided. Although there is a positive correlation between fluorescence production and aPDT efficiency, the optimum incubation time should not be too long [41].

To evaluate the dark toxicity, we found the survival of MRSA was not affected by ALA at all concentrations within 4 h, indicating ALA did not induce dark toxicity in MRSA cells. However, the number of viable colonies were partially inhibited by higher concentrations of ALA (5 mM and 50 mM) at 12 h. Although previous studies have found that the incubation of ALA at 5 mM or 10 mM in the dark for 1 h has a partial inhibitory effect, we consider that increasing acidification of the culture at high concentrations was reported to exhibit antibacterial activity as indicated in their discussion [24].

Through bactericidal experiments, we found that 4 h incubation time could produce significant sterilization effect at the lowest dose of 96 Jcm^{-2}. Therefore, 4 h was adopted as the optimal time, which is consistent with previous clinical studies [42]. Based on our preliminary experiments (data not shown), we found that if we adopted 1 h incubation time, we needed stronger energy than 96 Jcm^{-2} to achieve the corresponding bactericidal effect, which will inevitably prolong the irradiation time, leading to prolonged treatment time and increased pain in clinic.

Our study showed the antibacterial activity was more susceptible to ALA-PDT at the moderate concentrations, but the inactivation of bacterial cells at high concentrations of ALA was attenuated. MRSA was almost completely inactivated at the moderate concentration of ALA (0.05 mM) after irradiation of 384 Jcm^{-2}. This result was in agreement with previous studies and could be explained by our PSs uptake experiment [39,40].

What's more, the CFU analysis also displayed light-dose dependence and bacterial survival reduced with increasing the energy of radiation, which were consistent with the previous research [19,24,40]. When the energy of radiation changed from 96 Jcm^{-2} to 384 Jcm^{-2}, the antimicrobial effect was enhanced. Therefore, ALA-PDT exhibited excellent disinfection effect and is a useful approach that can eradicate the bacterial infections. Comparing the results of single light treatment group and L + S+ group (0.05 mM at 384 Jcm^{-2}), ALA can completely eliminate bacteria.

Admittedly, higher energy is not always suitable in clinical practice, as it sterilizes better but may affect normal cells. We found that ALA-PDT is very safe under certain conditions, which is consistent with a previous study that aPDT did not destroy 3T3 cells [19]. 192 Jcm^{-2} is an ideal parameter with significant bactericidal effect and no damage to normal cells. 384 Jcm^{-2} may also be considered in the treatment of some particularly severe infections, as it affects only a subset of host cells.

Our study also concentrated on the mechanism of action of ALA-PDT. DCFH-DA, a nonfluorescent cell-permeant compound, is hydrolyzed by intracellular endogenous esterase, and the de-esterification product can be converted into fluorescent compound DCF upon oxidation by ROS [17]. The bactericidal effect of PDI is mainly ascribed to the ROS, which can attack and break down the integrity of membranes, and kill organisms, causing irreversible alterations to cytoplasmic membranes, respiratory chains, as well as nucleic acid [25,43,44]. Our result showed that ALA-PDT treatment significantly elevate intracellular ROS levels. The results correlated with the CFU assay, suggesting that cells destruction induced by aPDT was intimately associated with intracellular ROS production [45].

It was suggested that aPDT treatment can change the internal and external structural integrity of cells and lead to cell death [46]. As membrane integrity is considered to be one criterion for distinguishing between living and dead bacterial strains. We used fluorescent nucleic acid stain and TEM to identify the morphological changes of MRSA following treatment of ALA-PDT. SYTO 9 (green) can enter all cells, while PI (red) can only penetrate compromised cell membranes [47]. The observation results were basically consistent with the panel method, and similar patterns have been reported with other PSs-

mediated aPDT [17]. TEM found that cell wall thickening, and nucleic acid was damaged, which might contribute to the cell inactivation. It can be concluded that the cytoplasmic content was affected in the presence of ALA following irradiation. The morphology suggested that the mechanism by which ALA-PDT inactivated bacteria was mainly cytoplasmic decomposition. Similar results were also reported in other studies [46,48].

SDS-PAGE and agarose gel electrophoresis assay showed that both proteins and genomic structure were changed, indicating that proteins and genomic DNA degradation in cells treated by aPDT. However, neither ALA nor the light irradiation alone affected the proteins and DNA of MRSA. These findings concurred with previous research, which also concluded that aPDT could degrade proteins and DNA [46,49]. MRSA strains produce extracellular thermally stable nuclease encoded by the *nuc* gene, which has been well used in many laboratories to identify *S. aureus* [50]. In our study, the expression of the *nuc* gene was downregulated, suggesting that process of PDI actually interfered with the gene expression. Other studies related to genes expression after PDI have been found in the literature, such as the downregulation expression of EFG1, CPH1, BCR1, TEC1, HWP1, and ALS3 [51]. Similarly, another study found that the expression of *rcpA* gene in *Aggregatibacter actinomycetemcomitans* was affected by aPDT using qRT-PCR assay [27].

In this study, we selected a clinical representative strain MRSA325, which did not involve other strains of MRSA. However, the MRSA strains infected in clinical practice are more complex, and further investigation is needed to expand the types of MRSA strains to make a comprehensive discussion. In the electrophoresis section, we did not specify specific proteins and genes, but only studied the total proteins and genomes damaged by aPDT. The mechanism remains to be uncovered in future studies. In addition, our study is limited to sterilization in vitro. Due to immune mechanism, the internal environment is more complicated, and the obtained parameters can be used as preliminary reference. Further animal investigations are needed to verify the safety and efficacy of ALA-PDT.

5. Conclusions

In summary, we demonstrated the ALA-PDT was efficacious in controlling planktonic MRSA SA325, confirming that ALA-PDT may be a promising therapy against antibiotic-resistant bacteria infection. Within the limited scope of this study, further experiments are needed to elucidate the mechanisms involved in bacterial damage by ALA-PDT, and in vivo studies are necessary to confirm the effect of ALA-PDT to meet all the requirements of clinical practice.

Declaration of Competing Interest

None.

Acknowledgments

We are grateful to PhD Mingquan Guo at Shanghai Public Health Clinical Center for providing the bacterial strain. This work was supported by the National Natural Science Foundation of China (81572671).

References

[1] A.H. Lee, S.Y. Cho, T.S. Yam, K. Harris, M.R. Ardern-Jones, Staphylococcus aureus and chronic folliculocentric pustuloses of the scalp - cause or association? Br. J. Dermatol. 175 (2) (2016) 410–413.
[2] C. Dunyach-Remy, C. Ngba Essebe, A. Sotto, J.P. Lavigne, Staphylococcus aureus toxins and diabetic foot ulcers: role in pathogenesis and interest in diagnosis, Toxins 8 (7) (2016).
[3] P. Peyrani, J. Ramirez, What is the best therapeutic approach to methicillin-resistant Staphylococcus aureus pneumonia? Curr. Opin. Infect. Dis. 28 (2) (2015) 164–170.
[4] S.D. Kobayashi, N. Malachowa, F.R. DeLeo, Pathogenesis of Staphylococcus aureus abscesses, Am. J. Pathol. 185 (6) (2015) 1518–1527.
[5] L. Huang, T. Dai, M.R. Hamblin, Antimicrobial photodynamic inactivation and photodynamic therapy for infections, Methods Mol. Biol. 635 (2010) 155–173.
[6] M. Saleem, M. Nazir, M.S. Ali, H. Hussain, Y.S. Lee, N. Riaz, A. Jabbar, Antimicrobial natural products: an update on future antibiotic drug candidates, Nat. Prod. Rep 27 (2) (2010) 238–254.
[7] S. Tejiram, L.S. Johnson, M. Mete, S. Desale, K. Johnson, J. Zhang, L.T. Moffatt, J.W. Shupp, Screening nasal swabs for methicillin resistant Staphylococcus aureus: a regional burn center's experience, Burns 43 (4) (2017) 771–779.
[8] H. Hanberger, S. Walther, M. Leone, P.S. Barie, J. Rello, J. Lipman, J.C. Marshall, A. Anzueto, Y. Sakr, P. Pickkers, P. Felleiter, M. Engoren, J.L. Vincent, Increased mortality associated with methicillin-resistant Staphylococcus aureus (MRSA) infection in the intensive care unit: results from the EPIC II study, Int. J. Antimicrob. Agents 38 (4) (2011) 331–335.
[9] F. Vatansever, W.C. de Melo, P. Avci, D. Vecchio, M. Sadasivam, A. Gupta, R. Chandran, M. Karimi, N.A. Parizotto, R. Yin, Antimicrobial strategies centered around reactive oxygen species–bactericidal antibiotics, photodynamic therapy, and beyond, FEMS Microbiol. Rev. 37 (6) (2013) 955–989.
[10] T. Tsai, Y. Yang, T.H. Wang, H.F. Chien, C. Chen, Improved photodynamic inactivation of gram-positive bacteria using hematoporphyrin encapsulated in liposomes and micelles, Lasers Surg. Med. 41 (4) (2010) 316–322.
[11] N. Chiniforush, M. Pourhajibagher, S. Shahabi, A. Bahador, Clinical approach of high technology techniques for control and elimination of endodontic microbiota, J. Lasers Med. Sci. 6 (4) (2015) 139.
[12] J. Giulio, F. Clara, S. Marina, F. Stefania, C. Olimpia, D. Donata, F. Lia, C. Giacomo, R. Gabrio, Photodynamic therapy in the treatment of microbial infections: basic principles and perspective applications, Lasers Surg. Med. 38 (5) (2010) 468–481.
[13] F.F. Sperandio, Y.Y. Huang, M.R. Hamblin, Antimicrobial photodynamic therapy to kill Gram-negative bacteria, Recent Pat. Antiinfect. Drug Discov. 8 (2) (2013) 108–120.
[14] R. van Hillegersberg, W.J. Kort, J.H. Wilson, Current status of photodynamic therapy in oncology, Drugs 48 (4) (1994) 510–527.
[15] H.-R. Jia, Y.-X. Zhu, Z. Chen, F.-G. Wu, Cholesterol-assisted bacterial cell surface engineering for photodynamic inactivation of Gram-positive and Gram-negative bacteria, ACS Appl. Mater. Interfaces 9 (19) (2017) 15943–15951.
[16] A.S. Garcez, S.C. Núnez, N. Azambuja Jr, E.R. Fregnani, H.M. Rodriguez, M.R. Hamblin, H. Suzuki, M.S. Ribeiro, Effects of photodynamic therapy on Gram-positive and Gram-negative bacterial biofilms by bioluminescence imaging and scanning electron microscopic analysis, Photomed. Laser Surg. 31 (11) (2013) 519–525.
[17] B. Mai, Y. Gao, M. Li, X. Wang, K. Zhang, Q. Liu, C. Xu, P. Wang, Photodynamic antimicrobial chemotherapy for Staphylococcus aureus and multidrug-resistant bacterial burn infection in vitro and in vivo, Int. J. Nanomed. 12 (2017) 5915–5931.
[18] L.P. Rosa, F.C.D. Silva, S.A. Nader, G.A. Meira, M.S. Viana, Effectiveness of antimicrobial photodynamic therapy using a 660 nm laser and methyline blue dye for inactivating Staphylococcus aureus biofilms in compact and cancellous bones: an in vitro study, Photodiagn. Photodyn. Ther. 12 (2) (2015) 276–281.
[19] K. Morimoto, T. Ozawa, K. Awazu, N. Ito, N. Honda, S. Matsumoto, D. Tsuruta, Photodynamic therapy using systemic administration of 5-aminolevulinic acid and a 410-nm wavelength light-emitting diode for methicillin-resistant Staphylococcus aureus-infected ulcers in mice, PLoS One 9 (8) (2014) e105173.
[20] X. Li, H.W. Wang, X.L. Wang, L.L. Zhang, Photodynamic therapy mediated by 5-aminolevulinic acid on inhibition of Staphylococcus epidermidis in vitro, Chin. J. Dermatol. 45 (8) (2012) 557–560.
[21] M.A. Awan, S.A. Tarin, Review of photodynamic therapy, Surgeon 4 (4) (2006) 231–236.
[22] H. Frederick, P. Lynne, Photodynamic therapy based on 5-aminolevulinic acid and its use as an antimicrobial agent, Med. Res. Rev. 32 (6) (2012) 1292–1327.
[23] H. Shi, J. Li, H. Zhang, J. Zhang, H. Sun, Effect of 5-aminolevulinic acid photodynamic therapy on Candida albicans biofilms: an in vitro study, Photodiagn. Photodyn. Ther. 15 (2016) 40–45.
[24] C.M. Hsieh, Y.H. Huang, C.P. Chen, B.C. Hsieh, T. Tsai, 5-Aminolevulinic acid induced photodynamic inactivation on Staphylococcus aureus and Pseudomonas aeruginosa, J. Food Drug Anal. 22 (3) (2014) 350–355.
[25] I.B. Rosseti, L.R. Chagas, M.S. Costa, Photodynamic antimicrobial chemotherapy (PACT) inhibits biofilm formation by Candida albicans, increasing both ROS production and membrane permeability, Lasers Med. Sci. 29 (3) (2014) 1059–1064.
[26] Z.H. Jiao, M. Li, Y.X. Feng, J.C. Shi, J. Zhang, B. Shao, Hormesis effects of silver nanoparticles at non-cytotoxic doses to human hepatoma cells, PLoS One 9 (7) (2014) e102564.
[27] M. Pourhajibagher, N. Chiniforush, S. Shahabi, S. Sobhani, M.M. Monzavi, A. Monzavi, A. Bahador, Monitoring gene expression of rcpA from Aggregatibacter actinomycetemcomitans versus antimicrobial photodynamic therapy by relative quantitative real-time PCR, Photodiagn. Photodyn. Ther. 19 (2017) S1572100017302028.
[28] T. Vremera, L.S. Iancu, C. Logigan, E. Nastase, E. Miftode, C. Lunca, O. Dorneanu, Optimization of triplex real time PCR for detecting Staphylococcus aureus mecA, pvl and nuc genes, Roum. Arch. Microbiol. Immunol. 70 (2) (2011) 69–73.
[29] R. Insa, M. Marin, A. Martin, P. Martin-Rabadan, L. Alcala, E. Cercenado, L. Calatayud, J. Linares, E. Bouza, Systematic use of universal 16S rRNA gene polymerase chain reaction (PCR) and sequencing for processing pleural effusions improves conventional culture techniques, Medicine 91 (2) (2012) 103–110.
[30] A. Pan, S. Lorenzotti, A. Zoncada, Registered and investigational drugs for the treatment of methicillin-resistant Staphylococcus aureus infection, Recent Pat. Antiinfect. Drug Discov. 3 (1) (2008) 10–33.
[31] B. Thakuria, K. Lahon, The beta lactam antibiotics as an empirical therapy in a

developing country: an update on their current status and recommendations to counter the resistance against them, J. Clin. Diagn. Res. 7 (6) (2013) 1207–1214.
[32] A. Kawczyk-Krupka, B. Pucelik, A. Miedzybrodzka, A.R. Sieron, J.M. Dabrowski, Photodynamic therapy as an alternative to antibiotic therapy for the treatment of infected leg ulcers, Photodiagn. Photodyn. Ther. 23 (2018) 132–143.
[33] F. Giuliani, M. Martinelli, A. Cocchi, D. Arbia, L. Fantetti, G. Roncucci, In vitro resistance selection studies of RLP068/Cl, a new Zn(II) phthalocyanine suitable for antimicrobial photodynamic therapy, Antimicrob. Agents Chemother. 54 (2) (2010) 637–642.
[34] G. Jori, C. Fabris, M. Soncin, S. Ferro, O. Coppellotti, D. Dei, L. Fantetti, G. Chiti, G. Roncucci, Photodynamic therapy in the treatment of microbial infections: basic principles and perspective applications, Lasers Surg. Med. 38 (5) (2006) 468–481.
[35] G.B. Kharkwal, S.K. Sharma, Y.Y. Huang, T. Dai, M.R. Hamblin, Photodynamic therapy for infections: clinical applications, Lasers Surg. Med. 43 (7) (2011) 755–767.
[36] R.A. Romano, S. Pratavieira, A.P.D. Silva, C. Kurachi, F.E.G. Guimarães, Light-driven photosensitizer uptake increases Candida albicans photodynamic inactivation, J. Biophoton. 10 (11) (2017).
[37] K.Q. Zhao, Y. Wu, Y.X. Yi, S.J. Feng, R.Y. Wei, Y. Ma, C.Q. Zheng, D. Qu, An in vitro model to study the effect of 5-Aminolevulinic acid-mediated photodynamic therapy on Staphylococcus aureus biofilm, J. Vis. Exp. (2018) 134.
[38] Y. Nitzan, M. Salmon-Divon, E. Shporen, Z. Malik, ALA induced photodynamic effects on gram positive and negative bacteria, Photochem. Photobiol. Sci. 3 (5) (2004) 430–435.
[39] A. Casas, H. Fukuda, G. Di Venosa, A. Batlle, Photosensitization and mechanism of cytotoxicity induced by the use of ALA derivatives in photodynamic therapy, Br. J. Cancer 85 (2) (2001) 279–284.
[40] N. Fotinos, M. Convert, J.C. Piffaretti, R. Gurny, N. Lange, Effects on gram-negative and gram-positive bacteria mediated by 5-aminolevulinic acid and 5-aminolevulinic acid derivatives, Antimicrob. Agents Chemother. 52 (4) (2008) 1366–1373.
[41] F. Hu, S. Xu, B. Liu, Photosensitizers with aggregation-induced emission: materials and biomedical applications, Adv. Mater. 30 (45) (2018) e1801350.
[42] V. Nesi-Reis, D. Lera-Nonose, J. Oyama, M.P.P. Silva-Lalucci, I.G. Demarchi, S.M.A. Aristides, J.J.V. Teixeira, T.G.V. Silveira, M.V.C. Lonardoni, Contribution of photodynamic therapy in wound healing: a systematic review, Photodiagn. Photodyn. Ther. 21 (2018) 294–305.
[43] V. Adam-Vizi, Production of reactive oxygen species in brain mitochondria: contribution by electron transport chain and non-electron transport chain sources, Antioxid. Redox Signal. 7 (9–10) (2005) 1140–1149.
[44] J.S. Pan, M.Z. Hong, J.L. Ren, Reactive oxygen species: a double-edged sword in oncogenesis, World J. Gastroenterol. 15 (14) (2009) 1702–1707.
[45] L.D. Sordi, M.A. Butt, H. Pye, D. Kohoutova, C.A. Mosse, G. Yahioglu, I. Stamati, M. Deonarain, S. Battah, D. Ready, Development of photodynamic antimicrobial chemotherapy (PACT) for Clostridium difficile, PLoS One 10 (8) (2015) e0135039.
[46] X. Deng, S. Tang, Q. Wu, J. Tian, W.W. Riley, Z. Chen, Inactivation of Vibrio parahaemolyticus by antimicrobial photodynamic technology using methylene blue, J. Sci. Food Agric. 96 (5) (2016) 1601–1608.
[47] P. Stiefel, S. Schmidt-Emrich, K. Maniura-Weber, Q. Ren, Critical aspects of using bacterial cell viability assays with the fluorophores SYTO9 and propidium iodide, BMC Microbiol. 15 (2015) 36.
[48] Y. Wang, Q. Zhou, Y. Wang, J. Ren, H. Zhao, S. Wu, J. Yang, J. Zhen, Y. Luo, X. Wang, Y. Gu, In vitro photodynamic inactivation effects of Ru(II) complexes on clinical methicillin-resistant Staphylococcus aureus planktonic and biofilm cultures, Photochem. Photobiol. 91 (1) (2015) 124–133.
[49] J. Wu, H. Mou, C. Xue, A.W. Leung, C. Xu, Q.J. Tang, Photodynamic effect of curcumin on Vibrio parahaemolyticus, Photodiagn. Photodyn. Ther. 15 (2016) 34–39.
[50] I. Matouskova, V. Janout, Current knowledge of methicillin-resistant Staphylococcus aureus and community-associated methicillin-resistant Staphylococcus aureus, Biomedical papers of the Medical Faculty of the University Palacky, Olomouc, Czechoslovakia 152 (2) (2008) 191–202.
[51] F. Freire, P.P. de Barros, C.A. Pereira, J.C. Junqueira, A.O.C. Jorge, Photodynamic inactivation in the expression of the Candida albicans genes ALS3, HWP1, BCR1, TEC1, CPH1, and EFG1 in biofilms, Lasers Med. Sci. 33 (7) (2018) 1447–1454.